J.C.S. Faraday I, 1980, **76**, 2065–2079

Extraction of Rate Constant Distributions from Heterogeneous Chemical Kinetics

By Kevin F. Scott

Inorganic Chemistry Laboratory, Oxford University, South Parks Road, Oxford OX1 3QR

Received 7th September, 1979

The measured rate of a chemical process is often the sum of a series of individual rate processes. This paper outlines a computational method for the extraction of the distribution of rate constants in such a situation from the experimentally derived total rate plot against time. The method is tested using artificially generated data from given rate constant distributions and then applied to rate data obtained from reactions occurring on heterogeneous catalysts, to determine the site activity distribution functions prevailing on these surfaces. It constitutes, therefore, a means of quantifying the surface heterogeneity of a catalyst towards a reaction. Essential to the method are rate data of precision obtained under carefully controlled conditions, a requirement which is admirably fulfilled by carrying out the reaction in a chromatographic column using stopped-flow chromatography to measure reaction rates.

While the rate of a chemical reaction in a homogeneous medium is normally a simple function of the active masses of the interacting substances, a number of cases arise where the rate of the reaction is not so simply described in these terms and compensation for the variation of velocity constant among the reacting species must be made. An example of this is the total rate of disintegration of a mixture of radioactive isotopes, where the measured rate is the sum of a series of exponential decays. The phenomenon is also widely encountered in reactions on heterogeneous catalysts, where adsorbed reacting species should have rate constants depending on the activity of the catalytic site on which they are adsorbed. The object of the present work was to devise a method by which the rate of a reaction could be interpreted in terms of a distribution of rate constants, which we shall call the activity distribution function and to develop a computational method for its extraction from rate data.

We first consider the theory of the numerical method itself, test it using synthetic data from known distribution functions and then apply it to the particular case of certain heterogeneously catalysed reactions, for which the activity distribution functions can be extracted. Finally, several examples are given of the extraction of the activity distribution function in cases where the catalyst is operated at different temperatures, modified by a chemical poison or thermally sintered.

THEORY

Consider a kinetic process which consists of a series of species reacting with first-order kinetics but with a distribution of rate constant between them. We will assume that: (*a*) the reaction is irreversible, (*b*) once one of the species has reacted it is not replaced and (*c*) there is no redistribution of rate constant between the species. As will be seen below, these constraints are reasonable over a wide range of applications of the model.

We now define the activity distribution function $F(k)$ such that the fraction of species having a rate constant lying between k and $k+\mathrm{d}k$ is given by $F(k)\,\mathrm{d}k$. The total rate of production of product from unit total starting concentration is given by:

$$R(t) = \int_0^\infty k\,\mathrm{e}^{-kt}F(k)\,\mathrm{d}k. \tag{1}$$

The function $F(k)$ can therefore in principle be derived by inverting eqn (1) numerically and there are several methods for doing this.[1] These methods are satisfactory for theoretical functions, but with experimental data slight variation from the function as a result of experimental error causes large deviations of the inverse function and an alternative approach had to be sought. A more satisfactory method is to choose some analytic form for the function $F(k)$ with adjustable parameters, substitute into eqn (1), perform the integration and fit the data to the resultant function, finding the optimum values for the parameters. Thus, $F(k)$ could be chosen as one or more square-wave functions, with adjustable widths, heights and positions, perhaps as triangles, *etc.*; however, in the work described here, $F(k)$ is chosen as follows:

$$F(k) = \sqrt{\frac{2}{\pi}}\frac{A_1\exp\left[-(k-\bar{k}_1)^2/2\sigma_1^2\right]}{\sigma_1 k} + \sqrt{\frac{2}{\pi}}\frac{A_2\exp\left[-(k-\bar{k}_2)^2/2\sigma_2^2\right]}{\sigma_2 k} \tag{2}$$

where A_1, A_2, $\bar{k}_1$, $\bar{k}_2$, σ_1 and σ_2, are adjustable parameters. This function is considered capable of representing as wide a variety of shapes of distribution function as possible, while limiting the number of parameters to six (two height parameters A_1, A_2, two positions $\bar{k}_1$, $\bar{k}_2$ and two width parameters σ_1, σ_2). It has potentially two maxima and two minima and is capable of a wide range of curvature, being able to represent distribution functions ranging from two sharp spikes to a flat, uniform plateau. Using this function the rate equation becomes:

$$R(t) = A_1\exp\left[\sigma_1^2t^2/2-\bar{k}_1t\right]\operatorname{erfc}\left\{\frac{\sigma_1 t}{\sqrt{2}}-\frac{\bar{k}_1}{\sigma_1\sqrt{2}}\right\} + A_2\exp\left[\sigma_2^2t^2/2-\bar{k}_2t\right]\operatorname{erfc}\left\{\frac{\sigma_2 t}{\sqrt{2}}-\frac{\bar{k}_2}{\sigma_2\sqrt{2}}\right\}. \tag{3}$$

It remains to fit this function to the experimental rate data, in order to identify the optimum values of the six parameters which describe the distribution function. The method chosen for this work was the iterative Gauss–Newton method due to Peckham [2] and was implemented using a routine from the Numerical Algorithm Group, Fortran library, E04FAF.

The numerical method was first tested using synthetic data, generated artificially from known distribution functions. Sets of 50 values of $R(t)$ were generated from eqn (3) using parameter sets corresponding to a broad distribution and two narrow " spikes ", respectively. These values of $R(t)$ were multiplied by normally distributed pseudo-random numbers having a mean value of unity and standard deviations of 0.02-0.10. Thus sets of data were generated corresponding to a known distribution function but respectively deviating by different degrees of random error.

The numerical method was then applied to these sets of data, to extract the distribution functions from them, for comparison with the starting function. It was necessary to supply the routine with initial estimates of the solution; three sets of such estimates were employed, corresponding to narrow, intermediate and broad distributions and the iterative procedure allowed to continue for 200 iterations per set of estimates. In this way all the sets of synthetic rate data were treated identically

and the solutions which exhibited the smallest sum of squares of residuals are shown in table 1, together with the parameters of the original known distribution function. There is close correspondence between the parameter values of the original distribution function and those identified by the computational method with up to 10 % standard deviation applied to the rate data points. Clearly, the distribution function can only be identified with any certainty within the " experimental " range of measurement, which in this case was 3-150 min, thus giving an approximate range of rate constant 0.007-0.3 min^{-1}. Moreover, at the extremes of this range the number of experimental points involved is small and so the degree of precision is lower. This is apparent from table 1, where, although the sizes, A_1 and A_2, and the positions, k_1 and k_2, take values close to those of the original distribution and the same is true for the width σ_1, the value of the width of the second spike at the higher rate, σ_2, is less precisely defined, since this peak is on the edge of the experimental range.

TABLE 1.—RESULTS OF TESTING THE NUMERICAL METHOD WITH SYNTHETIC DATA

(*a*) DUAL NARROW SPIKE DISTRIBUTION

	standard deviation of applied error	A_1 /mol min^{-1}	A_2 /mol min^{-1}	$\bar{k}_1$ /min^{-1}	$\bar{k}_2$ /min^{-1}	σ_1 /min^{-1}	σ_2 /min^{-1}
starting distribution	—	1.0	1.0	0.01	0.10	0.002	0.002
	0.00	0.93	1.012	0.01	0.101	0.002	0.005
	0.02	1.035	0.894	0.011	0.084	0.0053	0.000 18
	0.04	0.789	1.313	0.0095	0.089	0.0036	0.103
	0.06	1.065	1.004	0.010	0.122	0.0016	0.018
	0.08	1.076	0.969	0.0123	0.095	0.0061	0.032 3
	0.10	1.04	1.028	0.0115	0.129	0.0055	0.007 4

(*b*) BROAD DISTRIBUTION

	standard deviation of applied error	A_1 /mol min^{-1}	A_2 /mol min^{-1}	$\bar{k}_1$ /min^{-1}	$\bar{k}_2$ /min^{-1}	σ_1 /min^{-1}	σ_2 /min^{-1}
starting distribution	—	1.0	1.0	0.05	0.1	0.05	0.05
	0.00	1.51	0.51	0.063	0.11	0.054	0.054
	0.02	1.09	0.193	0.044	0.1133	0.037	0.005
	0.04	2.27	0.072	0.08	0.192	0.063	0.0016
	0.06	0.50	1.55	0.041	0.099	0.03	0.073
	0.08	0.265	1.79	0.059	0.073	0.029	0.054
	0.10	1.40	0.614	0.056	0.158	0.047	0.0006

Note also that although six parameters are required to describe the two narrow spike distribution and the solution in terms of parameter values is unique in this case, a broad distribution essentially requires fewer parameters to describe it with equivalent precision; consequently there is a number of solutions in the broad distribution case with different parameter values, which all result in very similar forms for the distribution function itself. All the solutions in table 1(*b*) therefore result in very similar forms for the actual distribution function.

In practice the computational method was most efficient in its convergence if two narrow distributions were chosen as initial estimates of the solution, regardless of the form of the actual distribution function. It was easier for the routine to widen distributions to obtain an optimum fit than to narrow them. Occasionally the routine would find a false minimum from which it could not exit, but in these cases the sum of squares of residuals was several orders of magnitude greater than that of a genuine solution, whose sum of squares of residuals could be related to the estimated error on the data. The routine invariably located a solution if (*a*) a minimum of three sets of initial estimates of the solution was used, reflecting as wide a range of possible forms of the distribution functions as possible, (*b*) the routine allowed at least 200 iterations per set of initial parameters and (*c*) at least 50 data points were used. Further discussion on the performance of the routine is presented below where the application to experimental rate data is considered.

EXPERIMENTAL

All kinetic measurements were carried out using a Pye-Unicam model 104 chromatograph, using 1.5 m glass columns with 0.4 cm i.d., either packed throughout their entire length with catalyst material, which usually exhibited chromatographic properties which were suitable for the very simple analyses required, or packed with chromatographic stationary phase (*e.g.*, Porasil A), having a short length (20 cm) of catalyst packed into the inlet end of the column.

Reactants were injected by syringe into the head of the column through a septum which was checked by replacement for kinetically controlled "bleeding" effects, which would otherwise have masked the genuine kinetics. A stop tap was placed in the carrier gas line close to the head of the column to allow the flow to be interrupted for the stop periods and the carrier gas (variously nitrogen, hydrogen, or 1 % hydrogen in nitrogen) was dried using freshly activated silica gel and, where necessary, oxygen was rigorously excluded using manganese (II) oxide.[3]

The catalysts used were as follows: the alumina was 80-100 mesh F.20 alumina (Phase Separations Ltd, Queensferry, Clwyd) and used without modification. The $Ni–SiO_2$ catalyst was 2 % w/w nickel metal on Porasil A (Phase Separations), prepared as described elsewhere.[4] The platinum–Al_2O_3 catalyst was KCE platinum catalyst RD290C (Kali Chemie Englehard Katalysatoren GmbH, Hannover). The bismuth molybdate selective oxidation catalyst was prepared according to the method of Batist.[5]

Before use the catalyst columns were conditioned in a stream of carrier gas at 400°C for at least 3 h, before cooling to the reaction temperatures. Temperature stability was important in this work and the ovens were allowed at least $\frac{1}{2}$ h at the reaction temperature before an experiment was commenced. The temperature stability was checked using a calibrated Comark thermocouple meter (Comark Electronics Ltd, Littlehampton, Sussex) and the drift in the experiments was observed to be < 0.3°C over a 5 h period.

Computation was carried out on ICL 1906A and ICL 2980 computers.

RESULTS AND DISCUSSION

EXTRACTION OF THE ACTIVITY DISTRIBUTION FUNCTION FROM THE KINETICS OF REACTIONS ON CATALYST SURFACES

The phenomenon of catalyst surface heterogeneity has been previously investigated using a variety of techniques. Some of the earliest work was the derivation of the

Elovich equation [6] which allows for a distribution of activation energy in the kinetically controlled adsorption of an adsorbate to a surface; however, in the most well-known form of the equation the activation energy is assumed to increase linearly with coverage. Roginskii [7] has derived a graphical method for the extraction of a distribution function for the heats of adsorption across a surface from the adsorption isotherm, although the precision of the method falls rapidly as the curvature of the distribution function increases. More recently a number of workers have employed temperature-programmed desorption to investigate the range of activation energy in the desorption or surface reaction of an adsorbate and this has been recently applied,[8] for example, to the study of the selective oxidation of hydrocarbons.

The numerical method described in this paper can be used to extract a site activity distribution function for a catalyst giving an alternative way of quantifying the surface heterogeneity which is complementary to, and extends, the methods described above. However, the method has the limitations mentioned earlier, that the reaction occurring on the catalyst surface must be essentially first-order, that there must be no redistribution of the reactant over the catalytic sites as the reaction progresses and that there must be available kinetic data of sufficient precision and volume.

In the experiments described here, the redistribution of reactant over the sites was considered insignificant, because the chromatographic retention time of the reactants was immeasurably large and no movement of the reactants down the column could be detected in the experimental timescale. The processes studied were not known to be first-order, since the true order was masked by the effects of surface heterogeneity, but it is reasonable to expect that a first-order model might be applicable for the following reasons: (*a*) reactants were in low concentration and therefore species on the surface were widely separated from one another. (*b*) The reactants were immobile and therefore isolated. [In one instance, the elimination reaction of propan-2-ol on γ-alumina (see below), it was shown [9] that if mobility of the reactant was promoted by the addition of water, causing the alcohol to move along the chromatographic column, the accompanying kinetics showed an order of unity, with an average rate constant arising from the continual redistribution of reactant over the active sites.] The final requirement of precise rate data was afforded by stopped-flow chromatography and we can now consider the application of this technique to the various catalytic systems.

The advent of stopped-flow chromatography [10] has brought increased precision to the study of the kinetics of heterogeneous catalytic reactions [4, 11] and has allowed the measurement of kinetics over a wide range of reactant surface concentration, under closely controlled conditions. The data obtained from the technique are useful in kinetic modelling and mechanistic elucidation,[4] but several workers [11] have found that the kinetics obtained by stopped-flow chromatography are not always straightforward to interpret. In particular, even when there is evidence that a reaction should exhibit first-order kinetics, it rarely does so and the rate plots on a logarithmic scale show a curvature which is convex towards the origin. This is illustrated in fig. 1.

Although this curvature has been attributed [11] to surface heterogeneity of the catalysts (the most probable explanation), it is advisable to consider other possible causes of the phenomenon before proceeding.

First, it could arise as a result of the inherent non-first-order behaviour of the reaction, *i.e.*, by some kind of inhibition, poisoning of the reaction or promotion of it by reactants or products or by a combination of both. That this is unlikely is shown by the wide range of reaction types which show the phenomenon. Specifically, in the kinetic results presented here it can be discounted because, as far as possible, the influence of excess of the reactant or product on the kinetics was checked and

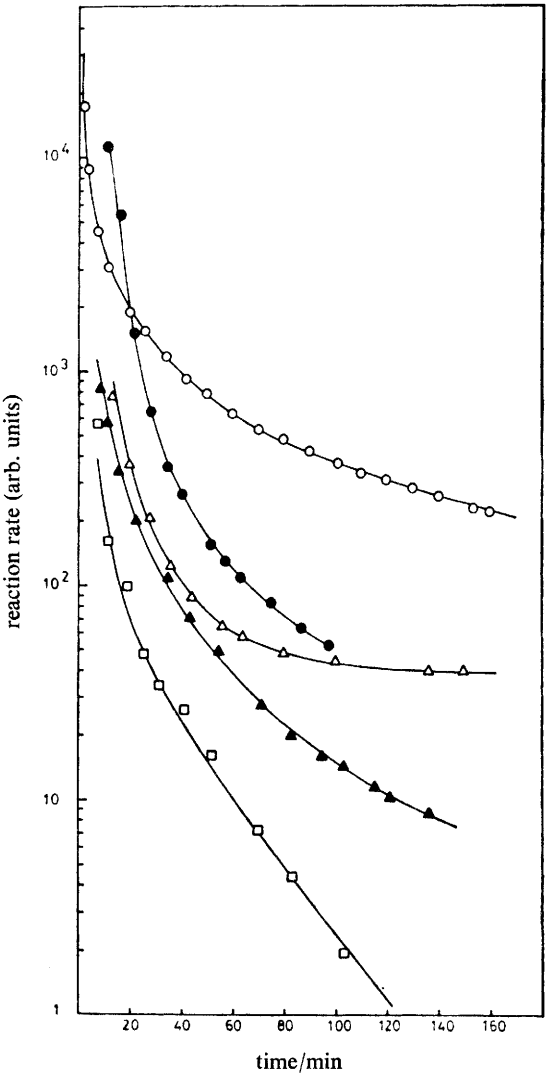

FIG. 1.—Rate plots obtained from stopped-flow chromatography. ○, Elimination of 2-chloropropane on alumina at 210°C. ●, Elimination of propan-2-ol on alumina at 237°C. ▲, Fischer-Tropsch reduction of carbon monoxide on Pt–Al_2O_3 at 180°C. △, Methanation step in the hydrogenolysis of n-hexane on Ni–SiO_2 at 150.9°C. □, Combustion of acrylic acid on Bi_2MoO_6 at 400°C.

found not to account for the curvature of the plots. Secondly, it is possible that the reactions are controlled by a surface diffusion phenomenon in which reactant adsorbed on to active sites reacts rapidly at the initial stages of the reaction and the curving profile is generated by diffusion of reactant from inactive areas of the catalyst to the active sites in a slower process. This was checked in the cases of reactions on alumina described here by introducing a second similar but distinguishable reactant during the course of a kinetic experiment, which was observed to continue unaltered by the new reactant. In this case, if the diffusion mechanism had prevailed, the addition of the second reactant would have occupied the active sites and inhibited

the product from the first reactant. We can conclude that this mechanism does not prevail here.

We return, therefore, to the conclusion that the curvature is due to the variation of site activity across the catalyst and now consider the application of the numerical method of experimental data.

EXPERIMENTAL TESTS OF THE METHOD

It was necessary to determine at the outset whether the method for extracting the site activity distribution function from the rate plot gave a physically meaningful result and to obtain an estimate of the power of the method to resolve between distribution functions of different shapes under experimental conditions. The physical significance of the distribution has been tested in a number of cases in which the effects of variation of temperature, poisoning of the catalyst surface and thermal sintering on the form of the distribution functions have been examined; these experiments are described in the following sections.

A major problem in the extraction of any function from its integral transform is that the integral is often insensitive to the detailed form of the function. Exhaustive tests were therefore carried out to ascertain whether the distribution functions obtained were unique solutions and whether the experimental data were able to resolve between distributions of different shapes.

The working range of the six-parameter space was searched thoroughly in each case by choosing 5 different sets of starting estimates of the parameters representing extremes of distribution shapes (from two narrow spikes to a continuous broad plateau) and performing a large number of iterations (usually 200) on each set of

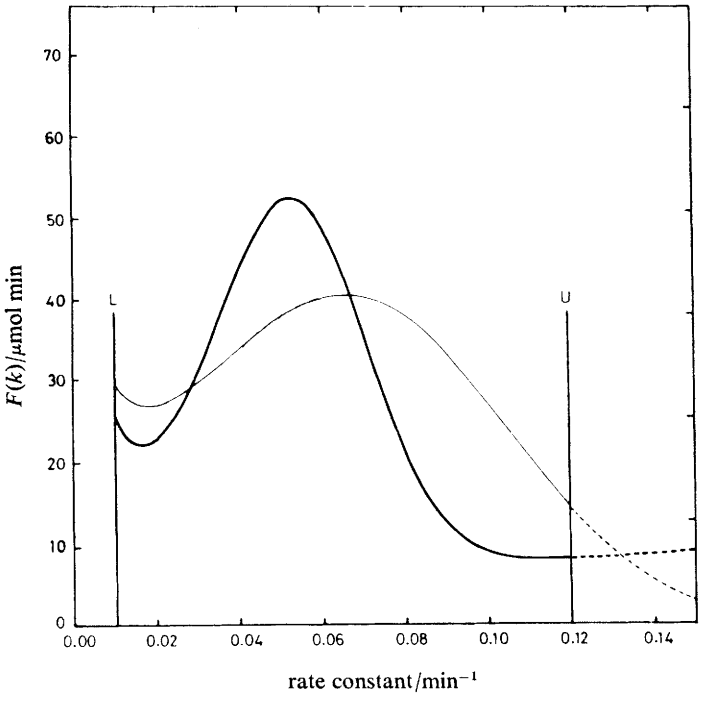

FIG. 2.—Site activity distribution functions for the Fischer–Tropsch reduction of carbon monoxide on Pt–Al_2O_3 at 180°C.

TABLE 2.—FINAL PARAMETERS FOR THE DISTRIBUTION FUNCTION OBTAINED FOR THE CO METHANATION ON $Pt-Al_2O_3$

A_1/mol min^{-1}	A_2/mol min^{-1}	$\bar{k}_1$/min^{-1}	$\bar{k}_2$/min^{-1}	σ_1/min^{-1}	σ_2/min^{-1}
5.27×10^{-8}	1.01×10^{-6}	0.059	0.409	0.0172	0.158

starting estimates. In this way a representation of a wide range of distribution shapes was examined and in each case a measure of the closeness of fit obtained in the form of the sum of squares of residuals. In every case tested, including all the data recorded in fig. 1, the form of the distribution function which gave a theoretical rate plot corresponding most closely to the experimental points was unique and no two distributions of disparate shape gave similar sums of squares for the same kinetic data set. Occasionally, as in the treatment of the synthetic data, the same distribution could be generated by different combinations of the 6 parameters, as might be expected, and in these cases plotting the distribution function in the experimental range of rate constant (0.01-0.25 min^{-1} in most cases) revealed the similarity of the functions.

One of the cases of greatest ambiguity encountered gave rise to the distributions in fig. 2, where distributions are shown for the kinetics of CO reduction on a platinum–alumina catalyst. In this experiment 1 cm^3 of gaseous carbon monoxide at 1 atm was injected on to a 1.5 m column containing the catalyst, maintained at 180°C and carrying a flow of hydrogen at 20 cm^3 min^{-1}. The rate of production of methane was followed by stopped-flow chromatography and the kinetic profile thus generated is shown in fig. 1. The form of the distribution function was extracted using the method above and during the course of the convergence > 1000 different distribution shapes were encountered. Finally, two solutions emerged, one having a root-mean-square deviation of 2.43 % shown by the heavy line in fig. 2 and the other having a root-mean-square deviation of 3.6 % shown by the light line. The range of rate constant accessible in the experiment is shown by the vertical lines marked U and L. An F-test was applied to determine the significance of one solution over the other and the result showed that the distribution given by the heavy line in fig. 2 was a better representation within 95 % confidence limits. The parameters which generated the final distribution are shown in table 2 and a comparison of the experimental and theoretical values for the rate plot shown in table 3.

EFFECT OF SELECTIVE POISONING OF A CATALYST SURFACE

The effect of partially poisoning a catalyst surface on the site activity distribution function obtained was investigated using an alumina catalyst. A 20 cm reactor column was packed with 0.253 g alumina, which was then activated in a stream of dry nitrogen overnight at 500°C and cooled to 58.5°C. An aliquot of 9.2×10^{-6} mol 2-chloro-2-methylpropane was injected on to the column and the production of 2-methylpropene followed by stopped-flow chromatography for ≈ 150 min using a β,β' oxydipropionitrile analytical column 2.5 m in length, at 0°C. The rate plot obtained in this way is shown using open circles to mark the experimental points in fig. 3. The column was then heated to 500°C for 3 h under nitrogen carrier gas and cooled to 200°C. It was then treated with 10 10-mm^3 aliquots of 2-chloropropane liquid in rapid succession and after 2 min the column rapidly cooled to 58.5°C. A further injection of 9.2×10^{-6} mol 2-methyl-2-chloropropane generated the rate plot marked with open triangles in fig. 3. Raising the temperature of the reactor to

TABLE 3.—COMPARISON OF EXPERIMENTAL AND CALCULATED VALUES FOR THE RATE OF CO REDUCTION ON $Pt–Al_2O_3$

time/min	rate of production of methane /10^8 mol min^{-1} experimental	calculated
8.6	19.59	19.96
11.65	13.54	12.73
15.55	8.05	8.37
18.55	6.52	6.51
22.60	4.81	4.90
25.60	3.99	4.08
29.55	3.33	3.28
34.60	2.57	2.54
37.60	2.24	2.21
40.60	2.02	1.94
43.55	1.66	1.71
46.55	1.48	1.51
51.60	1.28	1.25
54.60	1.15	1.12
57.60	1.02	1.01
60.60	0.948	0.911
64.60	0.805	0.803
67.60	0.730	0.734
70.60	0.648	0.673
73.60	0.606	0.620
76.60	0.556	0.573
79.60	0.517	0.531
82.60	0.481	0.494
85.60	0.452	0.461
88.60	0.426	0.432
91.60	0.423	0.405
94.55	0.380	0.382
100.6	0.346	0.341
103.6	0.334	0.324
106.6	0.314	0.308
109.6	0.299	0.294
112.6	0.285	0.280
115.6	0.273	0.268
118.6	0.260	0.257
121.6	0.242	0.247
124.6	0.241	0.237
127.6	0.232	0.229
130.6	0.224	0.221
133.6	0.210	0.213
136.6	0.202	0.206
139.6	0.194	0.200

200°C after the experiment generated a further kinetic profile of propene from the dehydrohalogenation of the 2-chloropropane and when this was exhausted the catalyst was restored to its original condition. The simplest explanation for the form of the profiles in fig. 3 is that the 2-chloropropane occupied the sites of lower activity, thus preventing the 2-chloro-2-methylpropane reaching them, thus rendering

the tail of the kinetic profile suppressed. The more active sites, however, are cleared of reactant during the short time at 200°C after treatment with the 2-chloropropane to give a rapid production of propane which was, in fact, observable as a sharp peak The distribution functions obtained from the kinetic plots are shown in fig. 4. The sites giving rise to reaction with rate constants in the range 0.01-0.08 min^{-1} are almost completely blocked with the slower poisoning reactant, while the faster species, on sites having a rate constant > 0.1 min^{-1}, remain present. Above 0.1 min^{-1} rate constant, the two distribution functions do not coincide. One possible reason for this is that when the slower sites are blocked the injected 2-chloro-2-methylpropane distributes itself over the remaining sites in such a way that the concentration on sites of intermediate activity is greater than on the unpoisoned surface. It is possible that these kinetic observations could be caused by a promoting effect in which the 2-chloropropane catalyses the reaction of 2-chloro-2-methylpropane on the slower sites, thus raising their rate constants and distorting the distribution accordingly. This was shown not to be the prevailing mechanism, since the injection of 2-chloropropane on to a catalyst previously treated with 2-chloro-2-methylpropane, in a separate experiment, had no effect on the kinetic profile of methylpropane from the latter reactant.

EFFECT OF THERMAL SINTERING

The effect of sintering of a catalyst on the distribution of activity was investigated using a Ni–SiO_2 catalyst to catalyse the Fischer–Tropsch reduction of CO to methane.

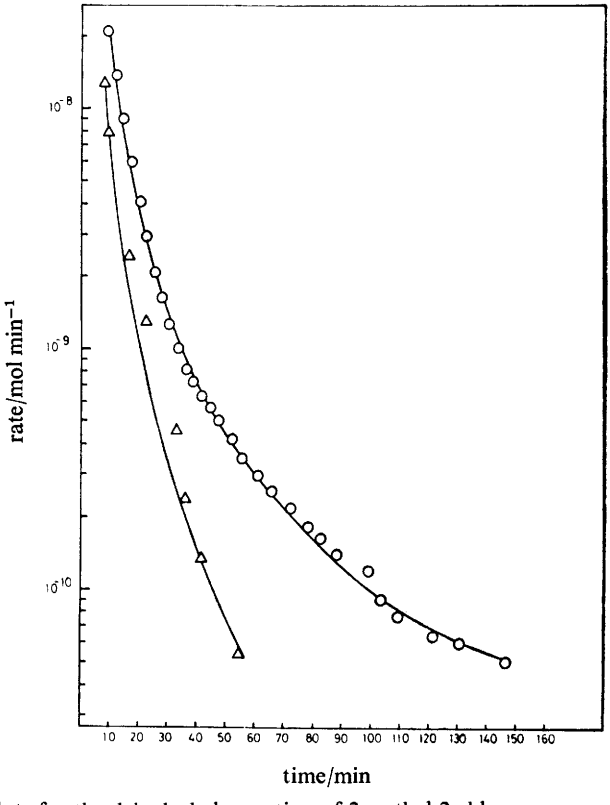

FIG. 3.—Rate plots for the dehydrohalogenation of 2-methyl-2-chloropropane on Al_2O_3 at 58.5°C, for ○, a freshly activated catalyst and △, a catalyst poisoned with 2-chloropropane.

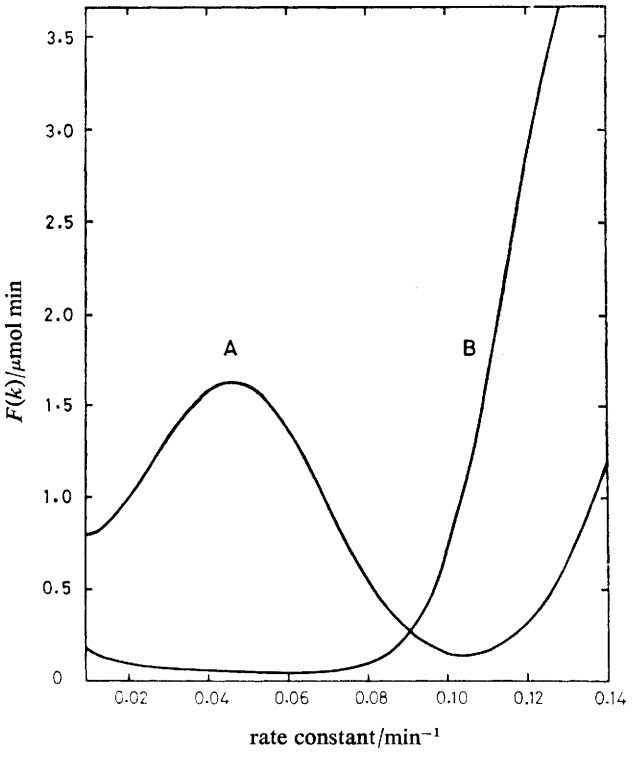

FIG. 4.—Site activity distribution functions for the dehydrohalogenation of 2-methyl-2-chloropropane on alumina for (*A*) the freshly activated catalyst and (*B*) the partially poisoned catalyst.

Samples of Ni–SiO_2 were subjected to sintering temperatures of 700, 800 and 1000°C, respectively, in a furnace in air for 105 min and the catalyst samples allowed to cool before packing into a short Pyrex reactor tube. Between 0.2-0.5 g of each was used and, after packing, the catalysts were conditioned at 400°C in a stream of hydrogen gas (22 cm^3 min^{-1} for 30 min). The reactor was then cooled to the reaction temperature (195°C) and 0.5 cm^3 CO at 1 atm was injected. The rate of production of methane was determined by stopped-flow chromatography, the analysis being carried out on a 1.5 m Porasil A column at the reaction temperature.

Fig. 5 shows the kinetic results. The characteristic curvature of the plots is observed, although the plot for the catalyst sintered at 700°C particularly shows appreciable linearity at the upper end. This has been attributed [12] to the inhibition of the reaction by large amounts of reactant on the catalyst surface and under favourable conditions the rate of production of methane has been observed to pass through a maximum. However, the general trends with increasing sintering temperature are that the curvature of the plots increases, the initial rate of reaction increases and the total amount of reaction decreases. These observations are also reflected in fig. 6 where the activity distribution functions for the catalysts are plotted. Here the distribution of activity becomes wider as sintering progresses, coupled with a shift to higher activity, and the total area under the distribution in the experimental range diminishes corresponding to a disappearance of sites. A number of processes could be responsible for these changes: the loss of sites is probably associated with the agglomeration of nickel crystallites and the dissolution of them into the silica support.

This was apparent particularly at the highest sintering temperature, where the catalyst changed colour from black to green and the black colour could not be restored by reduction with hydrogen at 400°C. It has been found [12] that all Ni–SiO_2 catalysts tend to accumulate carbonaceous species on their surfaces, which are very difficult to remove and which presumably cover some of the otherwise active sites. This is even the case on freshly prepared Ni–SiO_2 catalysts unless elaborate precautions are taken to prevent the introduction of carbonaceous materials (as adsorbates on the silica). The increase in the activity of the catalyst on sintering may be partly due to the uncovering of such sites by combustion of the carbonaceous species.

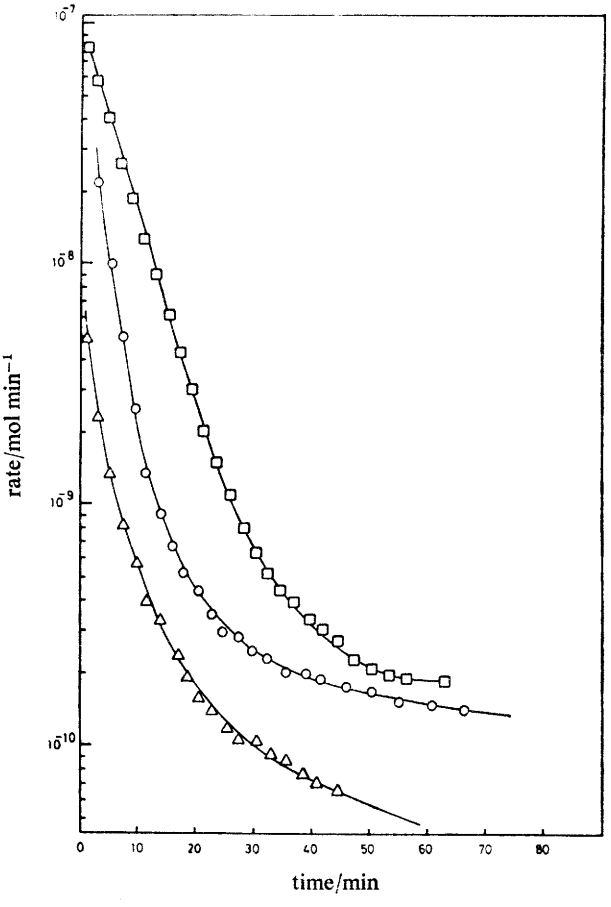

FIG. 5.—Rate plots for the Fischer–Tropsch reduction of carbon monoxide on Ni–SiO_2 at 195°C, on catalysts sintered at □, 700; ○, 800 and △, 1000°C.

EFFECT OF TEMPERATURE

The effect of temperature on the site activity distribution function was investigated in a series of experiments in which a 1.5 m dry alumina column was conditioned in a current of dry nitrogen for 12 h at 400°C and subjected to injections of 2-chloropropane (0.5 mm^3 liquid) at temperatures ranging between 175 and 225°C. In each case, the production of propene from the resultant dehydrohalogenation reaction was followed by stopped-flow chromatography. The kinetic plots are shown in fig. 7.

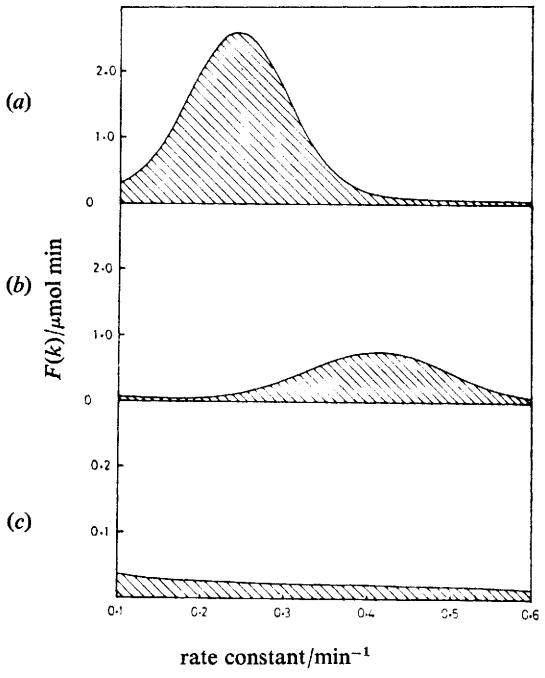

FIG. 6.—Site activity distribution functions for the Fischer–Tropsch methanation of CO on Ni–SiO_2 at 195°C, for catalysts sintered at (*a*) 700, (*b*) 800 and (*c*) 1000°C.

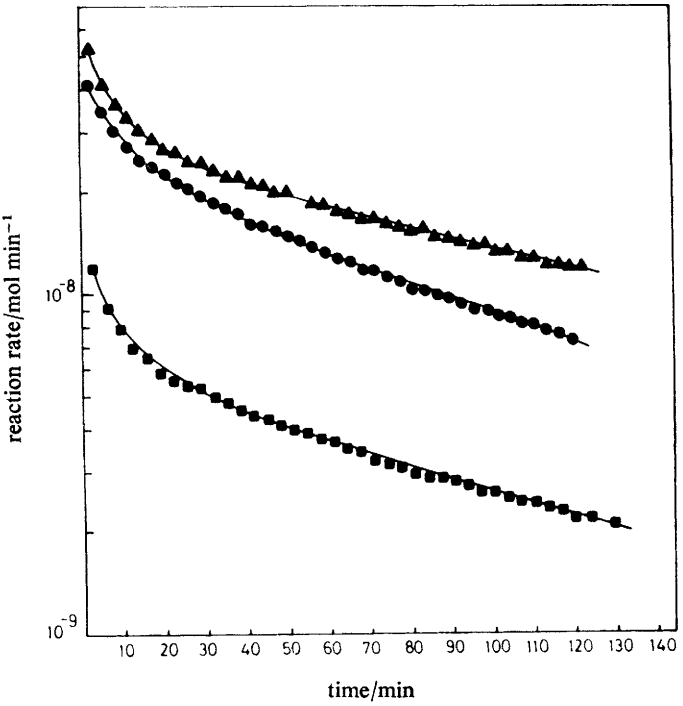

FIG. 7.—Rate plots for the dehydrohalogenation of 2-chloropropane on alumina, at ■, 175.4; ●, 199.8 and ▲, 225.4°C.

They show the expected curvature indicating variation in site activity and, although at all times during the experiments the actual values for the rates of production of propene increase with temperature as expected, it is not possible to obtain a value for the apparent activation energy for the reaction with any certainty since reliable slopes cannot be determined on the curved plots. In any case, as will be seen, such an apparent activation energy may have little physical significance.

The kinetic plots can be more readily understood when the adsorbate activity distribution functions are extracted using the computational method described above. The results are shown in fig. 8. They show a number of noteworthy features as follows:

(*a*) In general, as the temperature is raised, the area under the distribution function increases in the experimental range. This is a measure of the total number of adsorbate molecules reacting in the experimental time period and, as the temperature is raised, species of low activity and outside the experimental range at the lower temperature become observable, while species of higher activity move out of the experimental range. This is indicated by the arrows in fig. 8. The number of species in the experimental range then varies according to these effects and can be complicated to interpret.

(*b*) As the temperature is raised not only the number of species in the experimental " window " alters but also their Arrhenius parameters, since different species are in the window at different temperatures. This means that the apparent activation energies measured from such plots may have little significance in extreme cases such as this.

(*c*) The shape of the distribution function at 175.4°C and also that for the reaction of 2-chloro-2-methylpropane at 58.5°C in fig. 4, shapes which have been commonly

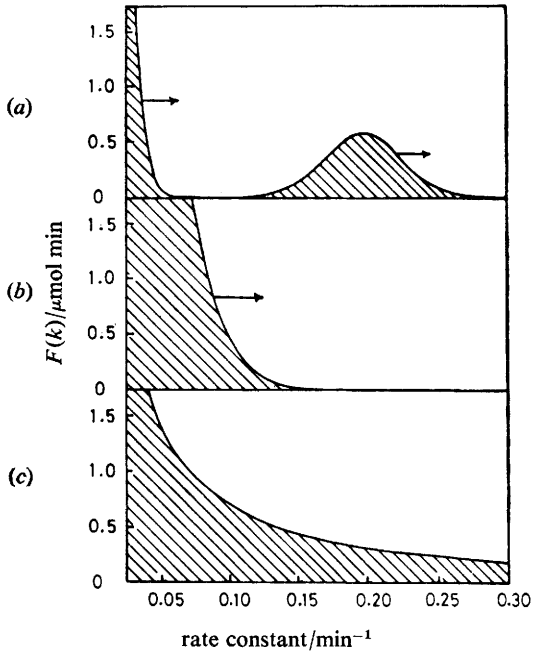

FIG. 8.—Site activity distribution functions for the dehydrohalogenation of 2-chloropropane on alumina, at (*a*) 175.4, (*b*) 199.8 and (*c*) 225.4°C.

observed for elimination reactions on alumina, give an indication of why attempts to explain the kinetics on a two site model have met with some success, since in these cases there are regions of high and low activity separated by a valley. Although this can be due to the existence of two types of site on the surface, having chemical differences rather than merely degrees of activity, this is not necessarily so. Merely a distribution of activation energy over the species, such that the more active have a lower activation energy (an entirely reasonable hypothesis), can result in a valley in the distribution function. This is because, as the temperature is lowered, species of lower activity and higher activation energy move downward in activity faster than those of higher activity and lower activation energy. This can cause a sparsely populated mid-activity region.

We can conclude from this work that the rate plots from stopped-flow chromatography are capable of generating a form of the distribution function for adsorbate activity whose general shape is well defined and which changes coherently with changes in experimental conditions, with catalyst pretreatment and from catalyst to catalyst. It is therefore introduced as a further approach to the understanding of catalyst surfaces and as a means of accounting for heterogeneity when modelling catalytic kinetics in mechanistic investigations.

I acknowledge the support of the Petroleum Research Fund of the American Chemical Society and extend grateful thanks to Drs. A. Cox, C. S. G. Phillips and J. Rollett for many useful discussions.

[1] R. Herschel, *A Guide to the Application of the Laplace and Z transforms* (Van Nostrand Reinhold, London, 1971), p. 138.
[2] G. Peckham, *Computer J.*, 1970, **13,** 418.
[3] C. R. McIlwrick and C. S. G. Phillips, *J. Phys. E*, 1973, **6,** 1208.
[4] K. F. Scott, M. A. Abdulla and F. H. Hussein, *J.C.S. Faraday I*, 1978, **74,** 2873.
[5] Ph. A. Batist, *J. Catalysis*, 1976, **41,** 333.
[6] S. Yu. Elovich and S. Z. Roginskii, *Acta Physicochim. U.S.S.R.*, 1937, **3,** 595.
[7] S. Z. Roginskii, *Adsorbciya i Kataliz na Neodnorodnykh Poverkhnotsyyakh* (Izd. Acad. Nauk S.S.S.R., Moscow, 1948).
[8] L. D. Krenzke, G. W. Keulks, A. V. Skylarov, A. A. Firova, M. Yu. Kutirev, L. Ya. Margolis and O. V. Krylov, *J. Catalysis*, 1978, **52,** 418.
[9] I. Z. Karabassis, *D.Phil. Thesis* (Oxford University, Oxford), in preparation.
[10] C. S. G. Phillips, A. J. Hart-Davis, R. G. L. Saul and J. Wormald, *J. Gas Chromatogr.*, 1967, **5,** 424.
[11] N. A. Katsanos and I. Hadzistelios, *J. Chromatogr.*, 1975, **105,** 13.
[12] J. Wolstenholme, *Pt. II Thesis* (Oxford University, Oxford, 1974).

(PAPER 9/1434)